Modeling, Simulation and Implementation of Brushed DC Motor Speed Control Using Optical Incremental Encoder Feedback

Bharat Joshi[1], Rakesh Shrestha[2], Ramesh Chaudhary[3]

[1,2] *Department of Electronics and Computer Engineering, IOE, Central Campus, Pulchowk, Tribhuvan University, Nepal*

[3] *Department of Mechanical Engineering, IOE, Central Campus, Pulchowk, Tribhuvan University, Nepal*

Corresponding Email: 067bex408@ioe.edu.np

Abstract: Brushed DC motors are widely used in industrial applications where speed regulation requirements are critical. Speed control of DC motor using incremental optical encoder feedback mechanism and Simulink model of DC Motor is presented in this paper. Quadrature decoding of encoder pulses is done to measure motor speed at a sampling instant and PID controller algorithm is applied to compute control variable in the form of PWM. Motor driver, here the H-bridge circuit, responds to the PWM signal and produces voltage proportional to PWM duty cycle that actuates DC motor resulting in motor speed proportional to PWM duty cycle. Experiments show that proper tuning of PID parameters result in smooth tracking of the reference speed.

Keywords: PID control; H-bridge; DC Motor; Optical Encoder

1. Introduction

DC motor drives are used for many speed and position control systems where their excellent performance, ease of control and high efficiency are desirable characteristics. Brushed DC (BDC) motors are widely used in applications requiring adjustable speed, good speed regulations and frequent starting, breaking and reversing. The speed of a BDC motor is proportional to the voltage applied to the motor. When using digital control, a pulse-width modulated (PWM) signal is used to generate an average voltage. The motor winding acts as a low pass filter, so a PWM waveform of sufficient frequency will generate a stable current in the motor winding. Though speed is proportional to PWM duty cycle, in systems where precise speed control is required, some sort of feedback mechanism must be included. Optical incremental encoders are widely used to provide position measurements in control systems at fixed sampling frequency. Encoder feedback implemented in combination with PID controller regulates the DC motor speed in response to load disturbances and noise.

PID controller has been used in industrial control applications for decades. PID controller has the ability to eliminate steady-state offsets through integral action, correct present error through proportional action, and it can anticipate the future through derivative action. The objective of a PID controller in a DC motor speed control system is to maintain speed at a given reference value and be able to accept new set point values dynamically.

2. DC Motor Model

The speed and torque of the motor depend on the strength of the magnetic field generated by the energized windings of the motor, which depend on the current through them. The DC motor speed is given by the relation

$$N = K\frac{(V - I_a R_a)}{Z\emptyset} \quad (1)$$

where,

$$K = \frac{60A}{P} \quad (2)$$

R_a = armature circuit resistance

I_a = armature current

V = motor input voltage

$\emptyset$ = machine's total flux

Z = motor's impedance

Therefore adjusting the rotor voltage (and current) will change the motor speed. In armature control of separately excited DC motors, the voltage applied to the armature of the motor is adjusted to control motor speed without changing the voltage applied to the field [1].

The electric equivalent circuit of the armature and the free-body diagram of the armature controlled separately excited DC motor is shown in Figure 1:

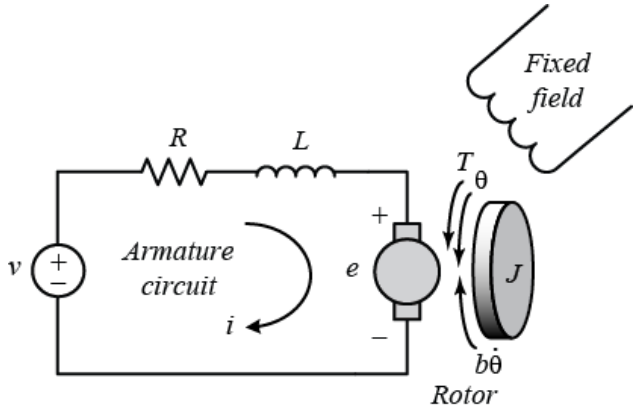

Figure 1: The electric equivalent circuit of the armature and the free-body diagram of the DC motor

Voltage source (V) applied to the motor's armature is considered as the input of the system; while the rotational speed of the shaft (dϴ/dt) is the output. The rotor and shaft are assumed to be rigid. It is further assumed that the system follows viscous friction model, that is, the friction torque is proportional to shaft angular velocity [2].

In general, the torque generated by a DC motor is proportional to the armature current and the strength of the magnetic field. It is assumed that the magnetic field is constant and, therefore, that the motor torque is proportional to only the armature current (I) by a constant factor motor torque constant, K_t as shown in the equation below.

$$T = K_t . I \quad (3)$$

This is referred to as an armature-controlled motor.

The back emf, e, is proportional to the angular velocity of the shaft by a constant factor back-emf constant, K_e.

$$e = K_e \dot{\theta} \quad (4)$$

In SI units, the motor torque and back emf constants are equal, that is,

$$K_t = K_e \quad (5)$$

Therefore, K is used to represent both the motor torque constant and the back emf constant.

From Figure 1, we can derive the following governing equations based on Newton's 2nd law and Kirchhoff's voltage law.

$$J\ddot{\theta} + b\dot{\theta} = Ki \quad (6)$$

$$L\frac{\partial i}{\partial t} + Ri = V - K\dot{\theta} \quad (7)$$

Applying the Laplace transform, the above modeling equations can be expressed in terms of the Laplace variable s.

$$s(Js + b)\theta(s) = KI(s) \quad (8)$$

$$(Ls + R)I(s) = V(s) - s\theta(s) \quad (9)$$

We arrive at the following open-loop transfer function by eliminating I(s) between the two above equations, where the rotational speed is considered the output and the armature voltage is considered the input.

$$T(s) = \frac{w(s)}{V(s)} = \frac{K}{(Js+b)(Ls+R)+K^2} \quad [\frac{rad/_{sec}}{V}] \quad (10)$$

3. Simulink Modeling, Simulation and Parameter estimation

Figure 2 represents Simulink block diagram of DC motor [3].

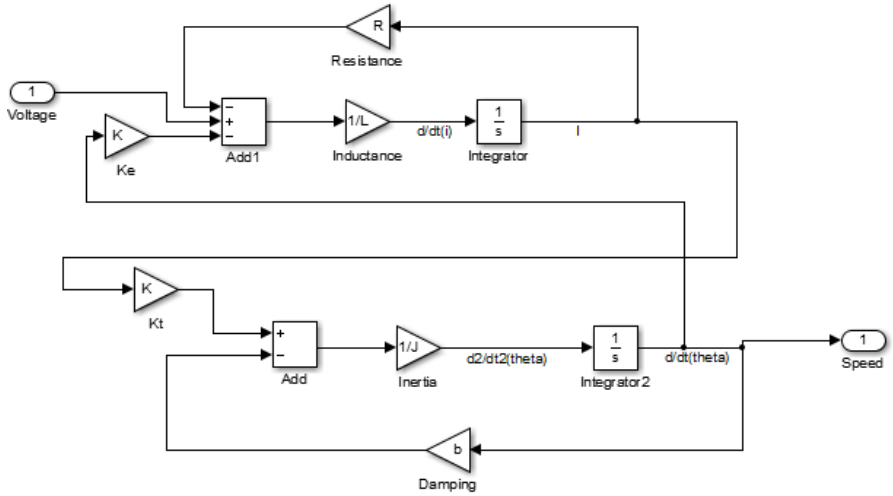

Figure 2: Simulink modeling of DC motor

Step response of the motor is as shown in Figure 3:

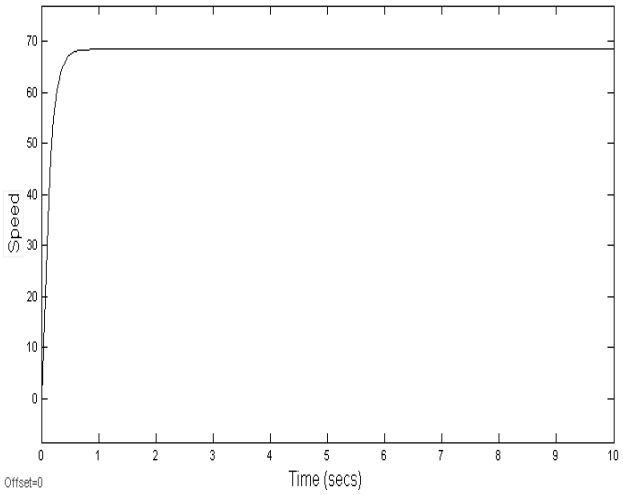

Figure 3: Step response of a DC motor

DC Motor parameter estimation is performed using MATLAB parameter estimation tool. Practically, some fixed input was applied to the DC motor and its response in terms of angular velocity was logged using incremental optical encoder mounted on motor shaft. The same input is applied to simulated DC motor in Simulink and its response is matched to that of DC motor used using non-linear least square method minimizing the sum of square errors as cost function.

Figure 4 shows the input voltage applied to motors (both practical and simulated)

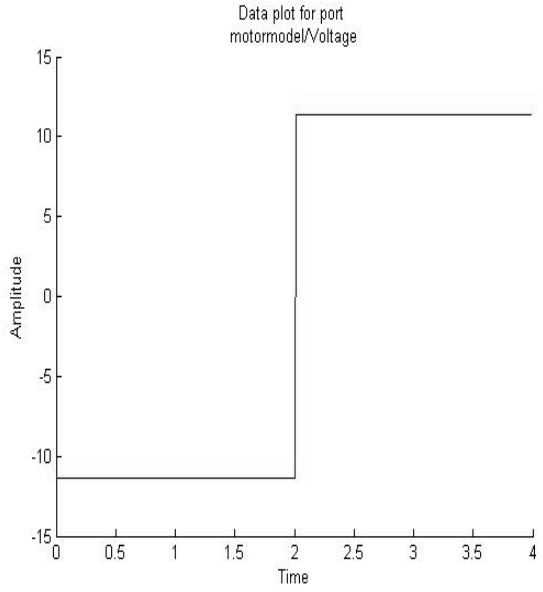

Figure 4: Motor Input Voltage plot

Figure 5 shows the response of practical VS simulated motor under same applied input voltage.

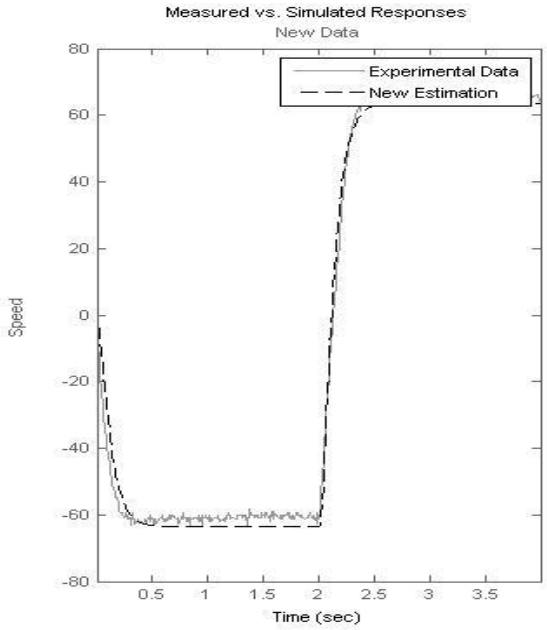

Figure 5: Measured VS Simulated Response of DC motor

The parameters obtained from non-linear least square matching were:

R = 8Ω

L = 0.2H

J = 0.00052

K = 0.17

b = 0.000115

4. Incremental Optical Encoder

Incremental encoders provide a specific number of equally spaced pulses per revolution (PPR) or per inch or millimeter of linear motion. Incremental encoders consist of three basic components: a slotted disc, a light source and a dual light detector, as shown in Figure 6. The light source shines on the disc, which has a regularly spaced radial pattern of transmissive and reflective elements, called encoder increments. The quadrature light detector measures the amount of light passed through the slotted disc and generates two quadrature output pulse signals, denoted by A and B. The up and down changes of the pulse signals are counted as a measurement of the encoder position [4].

Figure 6 shows the mechanism mentioned above:

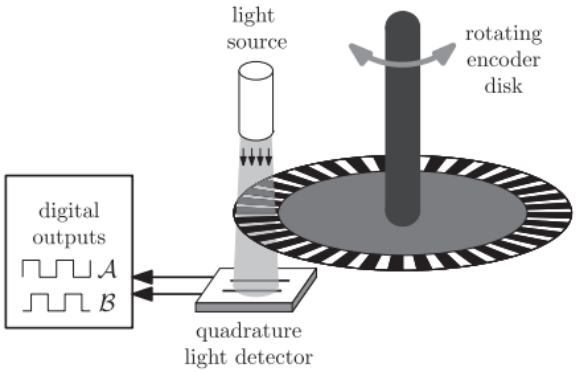

Figure 6: Underlying mechanism of incremental optical quadrature phase encoder

For the application of feedback control to motion systems with optical incremental encoders, the position is generally measured at a fixed sampling frequency. The measurement accuracy is limited by the quantization of the encoder, i.e., by the number of slits on the encoder disc. The quantization errors can be reduced by either using more expensive encoders with more increments or by using smart signal processing techniques. Furthermore, the position information of the encoders is distorted by several encoder imperfections, such as eccentricity and tilt of the disc, misalignment of the light detector/source, and a non-equidistant slit distribution. The quantization and encoder imperfections are performance limiting factors (PLFs) in optical incremental encoders. To improve velocity information obtained from optical incremental encoders; fixed time methods are used, which measures the traveled encoder counts over a fixed period-time. Counts are taken at particular sampling interval and try to control speed of DC motor to some reference input at that sampling time.

An encoder with one set of pulses is sometimes not sufficient because it cannot indicate the direction of rotation. Using two code tracks with sectors positioned 90 degree out of phase (as shown in Figure 7); the two output channels of the quadrature encoder indicate both position and direction of rotation. For example, if A leads B, the disk is rotating in a clockwise direction. If B leads A, the disk is rotating in a counter-clockwise direction. Therefore, by monitoring both number of pulses and the relative phase of signals A and B, the microcontroller can track both the position and direction of rotation. In addition, some quadrature encoders include a third output channel – called a zero or reference signal – which supplies a single pulse per revolution. This single pulse can be used for precise determination of a reference position. This signal is called the Z-Terminal or the index in most of encoder. A typical quadrature signal is shown in Figure 7:

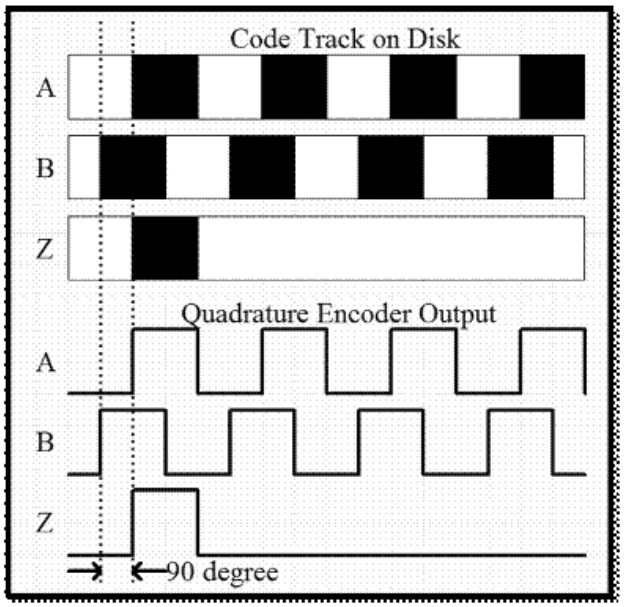

Figure 7: Typical quadrature signal

The quadrature incremental signals are typically decoded to obtain up to four times the base pulses per revolution (PPR). Quadrature decoding counts both the rising and falling edges of Channel A and B. Various quadrature decoding schemes are shown in Figure 8:

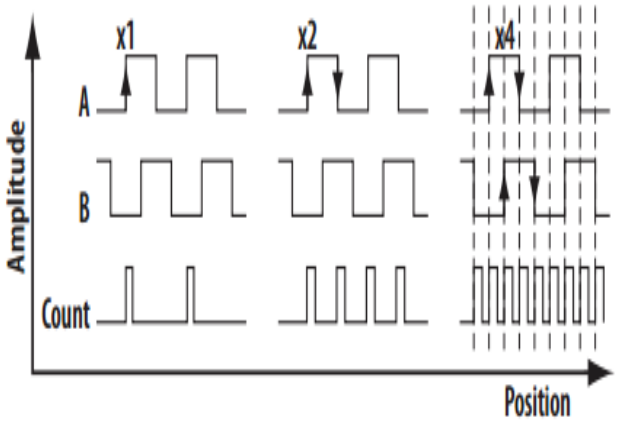

Figure 8: Decoding of quadrature phase signal

Encoder pulses during a sampling interval can be converted to motor speed using the equation:

$$C_m = \pi D_n / n C_e \quad (11)$$

where,

C_m = conversion factor that translates encoder pulses into linear wheel displacement

D_n = nominal wheel diameter (in mm)

C_e = encoder resolution (in pulses per revolution)

n = gear ratio of the reduction gear between the motor (where the encoder is attached) and the drive wheel

5. Motor driving

Effective armature voltage can be controlled by ON-OFF control only with Pulse Width Modulation (PWM) technique.

$$Duty\ cycle(\delta) = \frac{Pulse\ On\ time(\delta T)}{Pulse\ Time\ Period(T_{PWM})} \quad (12)$$

The relation between average voltage, supply voltage and duty cycle is given by:

$$V_{average} = \delta \times V_{supply} \quad (13)$$

The average voltage applied to the motor is proportional to the PWM duty cycle. This property of PWM can be used to smoothly vary the speed of the motor by changing the average value which is equivalent to changing the duty cycle of the signaling pulse. Both speed and direction control of the motor can be achieved using a PWM signal and the H-bridge.

Referring to Figure 9, MOSFET Q1 and Q2 make up one half-bridge while Q3 and Q4 make up the other half-bridge. Each of these half-bridges is able to switch one side of the BDC motor to the potential of the supply voltage or ground. When Q1 is turned on and Q2 is off, for instance, the left side of the motor will be at the potential of the supply voltage. Turning on Q4 and leaving Q3 off will ground the opposite side of the motor. The arrow labeled I_{FWD} shows the resulting current flow for this configuration.

The diodes across each of the MOSFETs (D1-D4) protect the MOSFETs from current spikes generated by back-EMF when the MOSFETs are switched off. These diodes are only needed if the internal MOSFET diodes are not sufficient for dissipating the back-EMF current.

The different drive modes for an H-bridge circuit are shown in Table 1. In Forward mode and Reverse mode, one side of the bridge is held at ground potential and the other side at V_{SUPPLY}. In Figure 9, the I_{FWD} and I_{RVS} arrows illustrate the current paths during the Forward and Reverse modes of operation. In Coast mode, the ends of the motor winding are left floating and the motor coasts to a stop. Brake mode is used to rapidly stop the BDC motor. In Brake mode, the ends of the motor are grounded. The motor behaves as a generator when it is rotating. Shorting the leads of the motor acts as a load of infinite magnitude bringing the motor to a rapid halt [5]. The I_{BRK} arrow illustrates this.

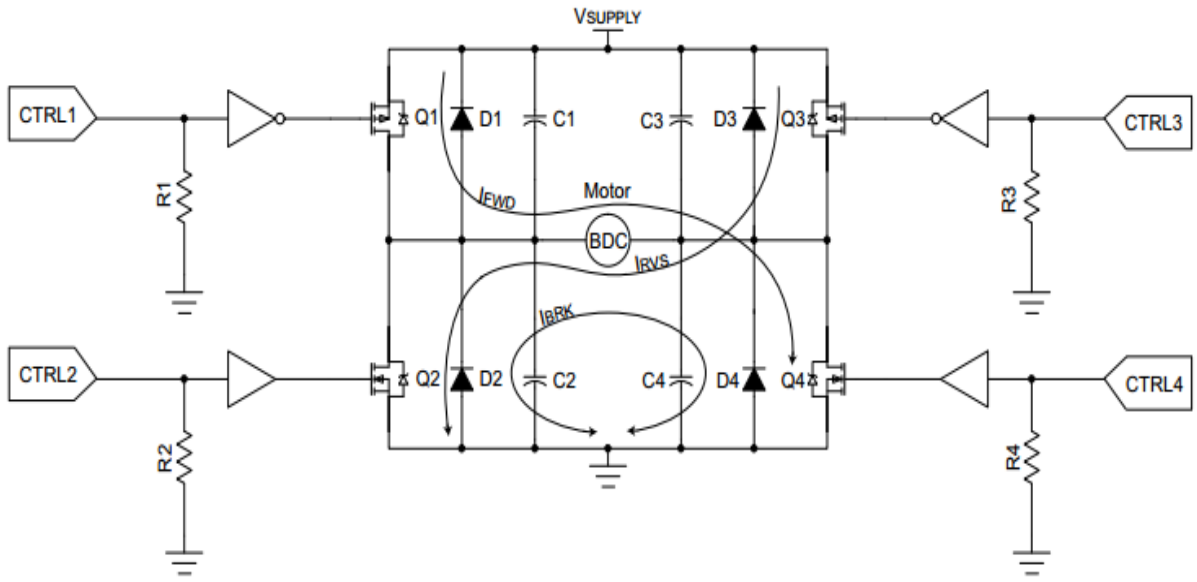

Figure 9: Basic H-bridge diagram

Table 1: Different H-bridge modes

	Q1	Q2	Q3	Q4
Forward	On	Off	Off	On
Reverse	Off	On	On	Off
Coast	Off	Off	Off	Off
Brake	Off	On	Off	On

Average motor current is a function of the electrical time constant of the motor, T_e.

Where,

$$T_e = \frac{L}{R} \quad (14)$$

The average pulse current will depend upon the ratio of the PWM period (T_{PWM}) to the motor electrical time constant, T_e.

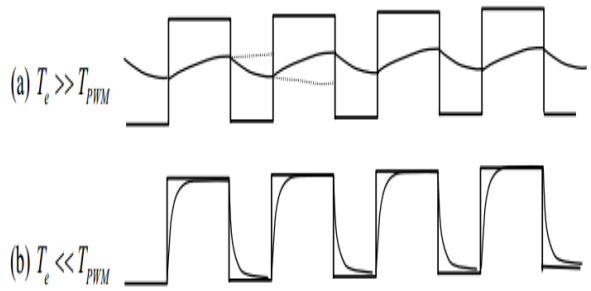

Figure 10: Current through a motor at different Electric Time Constant (T_e)

If electric time constant T_e is much larger than the PWM period, the actual current flowing to the motor armature is a smooth curve, as illustrated in Figure 10(a). In other words, the inductance works as a low-pass filter, filtering out the sharp ON-OFF profile of the input voltage. In contrast, if the electric time constant is too small, compared to the PWM period, the current profile becomes zigzag, following the rectangular voltage profile, as shown in Figure 10(b). As a result, unwanted high frequency vibrations are generated at the motor rotor.

In most instances a motor which has high armature inductance will require a lower PWM drive frequency in order to establish the required current levels, and hence develop the necessary torque. A low inductance motor allows the use of a high switching drive frequency thus resulting in an overall faster system response.

As the PWM frequency increases, the current driven to the motor becomes smoother, and the nonlinearity due to discrete switching disappears. Furthermore, high PWM frequencies cause no audible noise of switching. The noise disappears as the switching frequency becomes higher than the human audible range (20 KHz). Therefore, a higher PWM frequency is in general desirable. However, it causes a few adverse effects [6]. As the PWM frequency increases:

• Switching loss increases and MOSFET may over-heat.

• Harmful large voltage spikes and noise are generated.

• Radio frequency interference and electromagnetic interference become prominent.

In general, to achieve optimum efficiency in a PWM motor drive at the highest practical frequency, the motor should have an electrical time constant, T_e, close to the duration of the applied waveform T_{PWM}.

$$T_e = K \times T_{PWM} \quad (15)$$

where K is small.

Thus an appropriate choice of switching frequency and motor inductance ensures a high average motor current during each switching pulse. Motor current control, and hence torque control, is achieved by varying the period of the applied pulsed waveforms.

Torque is dependent on average motor current (equation 1) which, in turn, is controlled by PWM Time period.

$$\tau = K_t \times I \quad (16)$$

6. PID Controller

Load on the motor is subjected to change. Other factors such as age, environments etc. also affect the operation of the motor. Consequently, feedback mechanisms are typically employed to control the motor speed at a certain reference speed. Thus a PID control mechanism is implemented to stabilize the system in its original orientation. The tuning of the PID algorithm is a never-ending optimization process.

The PID tuning comprises of three parameters: P (proportional), I (integral) and D (differential) terms whose proper values maintain the stability of the whole system. A proportional controller (with proportional gain K_P) will have the effect of reducing the rise time and will reduce, but never eliminate, the steady-state error. An integral control (with integral gain K_i) will have the effect of eliminating the steady-state error, but it may make the transient response worse. A derivative control (with differential gain K_d) will have the effect of increasing the stability of the system, reducing the overshoot, and improving the transient response.

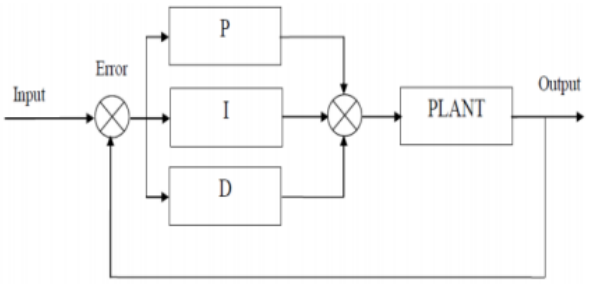

Figure 11: Block diagram of PID Controller

Heuristically, PID parameters can be interpreted in terms of time: P depends on the present error, I on the accumulation of past errors, and D is a prediction of future errors, based on current change. The weighted

sum of these three actions is used to adjust the process via a control (as shown in Figure 11)

Mathematical model of PID:

$$c(t) = K_P E(t) + K_I \int_0^t E(t)dt + K_D \frac{dE(t)}{dt} \quad (17)$$

Digital model of PID:

$$c(n) = K_P E(n) + K_I T_s \sum_0^N E(n) + K_D \frac{E(n) - E(n-1)}{T_s} \quad (18)$$

7. Implementation

On the DC motor, XYK-BMS-32Z6-C1024 encoder with a resolution of 1024 pulses per revolution (PPR) is mounted. The experimental setup consists of mechanical setup for brushed DC Motor along with feedback and motor driver circuitry (H-bridge) as shown in Figure 12.

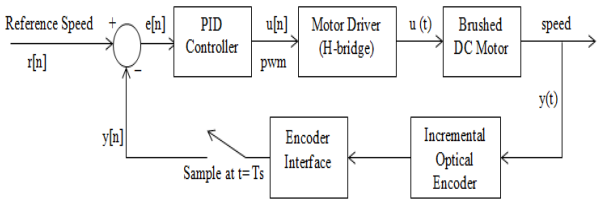

Figure 12: Experimental setup for brushed DC motor speed control

Discrete PID controller and encoder interfacing are implemented on ATMega8 microcontroller which performs encoder data acquisition at a given sampling frequency. A discrete PID controller reads the error, calculate and output the control input at a given time interval, at the sample period T. The sample time was chosen less than the shortest time constant in the system.

Using Parameter Estimation, electrical time constant (T_e) of DC motor was estimated to be 50ms.

Consequently, sampling time and PWM frequency were chosen 45ms and 16 KHz respectively.

Here, the reference signal r[n] indicates the desired motor speed where positive value indicates anticlockwise rotation and negative value indicates clockwise rotation. The quadrature input signals from optical encoder are fed to interrupt driven AtMega8 external interrupt pins to capture encoder events. The microcontroller counts no. of encoder pulses in the sampling interval and calculates motor rotational speed in Hz as,

$$Speed(Hz) = \frac{Count}{PPR \times T \times N} \quad (19)$$

where,

N = 1, 2 or 4 depending on type of quadrature decoding used as illustrated in Figure 8.

Count = No. of counts in sampling interval

PPR = Encoder resolution (Pulse Per Revolution)

T = sampling interval

Error at each sample instant is calculated and applied to PID controller which calculates the desired control variable in the form of PWM. Thus obtained PWM signal is applied to motor driver (H-bridge) that actuates the DC motor in such a way that motor speed is proportional to the PWM duty cycle. However, PID parameters (K_p, K_i and K_d) must be tuned for desirable system response and were tuned manually by observing the effect of change in PID constants on the system performance.

Integral Windup and Derivative Filtering

Motor has some speed limit and control variable (PWM) may reach the DC motor speed limit. When this happens the feedback loop is broken and the system runs as an open loop system because the motor will remain at its limit independently of the process output. If a controller with integrating action is used, the error may continue to be integrated if the algorithm is not properly designed. This means that the integral term may become very large or, colloquially, it may "wind up." The consequence is that any controller with integral action may give large transients when the motor saturates. Also high integral term results in sluggish PID controller response.

Simple integral anti-windup strategy can be implemented by limiting the integral term between MIN_I_TERM and MAX_I_TERM.

A caveat to derivative action is that an ideal derivative has very high output for high-frequency signals. This means that high-frequency measurement noise will generate large variations of the control signal. The effect of measurement noise to some extent can be eliminated by first order filtering of derivative term [7].

The complete digital PID algorithm implemented can be summarized as:

$$e[n] = r[n] - y[n] \quad (20)$$

$$P\_Term[n] = Kp \times e[n] \quad (21)$$

$$I\_Term[n] = I\_Term[n-1] + Ki \times e[n] \quad (22)$$

$$D\_Term[n] = (1-\alpha) \times D\_Term[n-1] - \alpha \times Kd \times (y[n] - y[n-1]) \quad (23)$$

$$I\_Term[n] = limiter(\text{I\_Term[n]}) \quad (24)$$

$$u[n] = base\_PWM + P\_term[n] + I\_Term[n] + D\_term[n] \quad (25)$$

The closed loop response of the system with PID controller is as shown in Figure 13, 14 and 15.

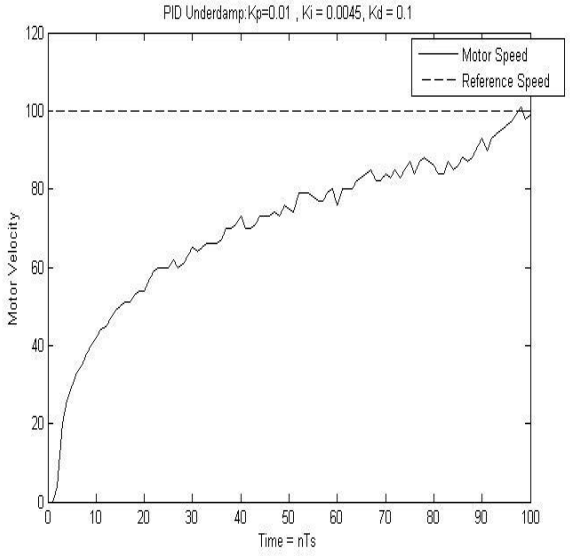

Figure 13: . Overdamped response

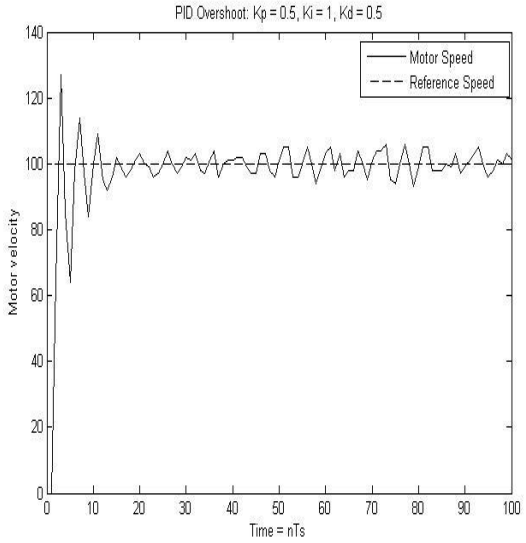

Figure 14: Response with Overshoot

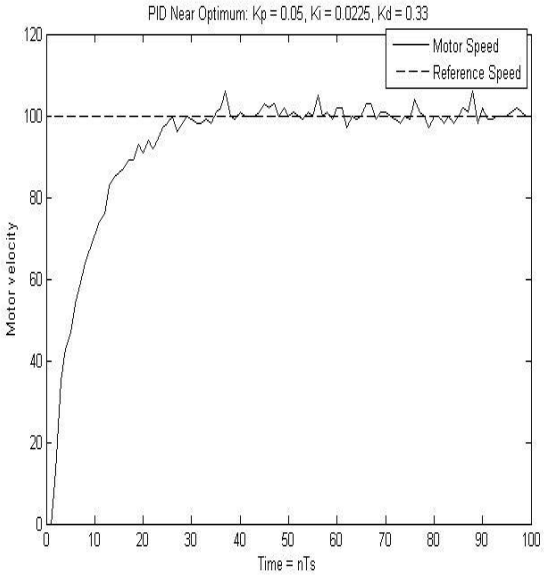

Figure 15: Near optimum response

8. Conclusion

In armature controlled separately excited DC motor, rotational speed is proportional to armature voltage. However, due to load disturbances, mechanical wear and tear and other environmental factors DC motor response varies with time. To precisely regulate motor speed, we purpose to use PID controller based feedback mechanism with incremental optical encoder as speed measurement sensor.

Incremental encoder feedback mechanism involves quadrature phase decoding of signals A and B; and decoded position data or encoder count is sampled at sample period T_s to obtain DC motor velocity. This velocity acts as feedback to the PID controller which acts on error between reference signal and feedback to produce required PWM signal as control variable. Thus obtained PWM signal is applied to H-bridge that actuates DC motor with motor speed proportional to PWM duty cycle. Experiments show that careful tuning of PID parameters result in smooth tracking of reference speed and good speed regulation.

9. Future Enhancements

Future research involves reduction of systematic and non-systematic errors in encoder data. The main error sources in measured encoder signal are cycle error, pulse width error, phase error and eccentricity error. Optimization and automatic tuning of PID parameters also require future research.

References

[1] Sailan K., Kuhnert I.(2013). DC Motor Angular Position Control using PID Controller for the purpose of controlling the Hydraulic Pump. International Conference on Control, Engineering and Information Technology (CEIT'13), 2-6.

[2] Theraja B., Theraja A.(2011). A Textbook of Electrical Technology (Volume II- AC and DC machines). S. Chand, 995-1020.

[3] Saeed S.(2010). Automatic Control Systems. Katson Books, 46-48.

[4] Merry R., Molengraft M., Steinbuch M.(2013). Optical higher-order encoder time-stamping. IFAC (International Federation of Automatic Control) journal: Mechatronics – The science of intelligent machine, 1-3.

[5] Condit R.(2010). Brushed DC Motor Fundamentals. Microchip Application Note (AN905), 3-5.

[6] Asada H.(2005). Chapter 2: Actuators and Drive systems, Introduction to Robotics. MIT Open Courseware, 7-10.

[7] Astrom K., Hagglund T.(2006). Advanced PID Control, Instrumentation, systems, and Automation Society, 420-440.